Comparison of Sinusoidal and Space Vector PWM Control Techniques for Three-Level Inverter Drives

Ayse KOCALMIS BILHAN[1]
Sedat SUNTER[2]

Abstract
In recent years, inverters have been the most popular part of electrical drivers in variable voltage and frequency applications. Also multilevel inverters have gained interest in high power applications because of their advantages in high voltage and high power levels with low harmonic content. In this paper, basic structure of three-level inverter is introduced and its two modulation strategies are compared. One of the modulation algorithms is SPWM (Sinusoidal Pulse Width Modulation) technique where a sinusoidal modulation signal is compared with two triangle signals to obtain the three-level at the output phase voltage of the inverter. A simple SVPWM (Space Vector Pulse Width Modulation) algorithm is also realized. In this technique, three nearest vectors can be selected easily and switching sequence and switching times are calculated by using the vector position. Both techniques are simulated by using MATLAB/Simulink package program and applied to the RL and motor loads. Comparative results are given.

Keywords: *Inverters, pulse width modulation inverters, space vector pulse width modulation*

1. Introduction

In industries, where variable speed drives are required, induction motor drives are important. There are vairous strategies for control such as scalar control, vector control or field oriented control. In the literature, the inverters with having three levels or more than three levels on their output phase voltages have been named as multilevel inverters [1-3]. Multilevel inverters (MLs) have been usually applied to high power medium voltage applications due to their low switching frequency and less total harmonic distortion (THD) [1, 4]. Voltage stress of the each switching device is reduced because of the voltage share on the circuit. Besides, their harmonic content is reduced in higher levels. For example, three-level structure has less harmonic content than that of two-level structure at the same switching frequency [4, 5]. A schematic diagram of an H-Bridge multilevel inverter is shown in Fig.1. Three-phase output voltage waveforms are generated by various switching combination of the switches in the H-bridge inverter. As a result, three-level at the output phase voltage waveforms is obtained as +E/2 V, 0 V, -E/2 V. Number of H-bridges of each phase can be increased for getting higher levels. Number of H-bridges for each phase can be calculated using Eq. (1). (where; m is number of the output voltage level).

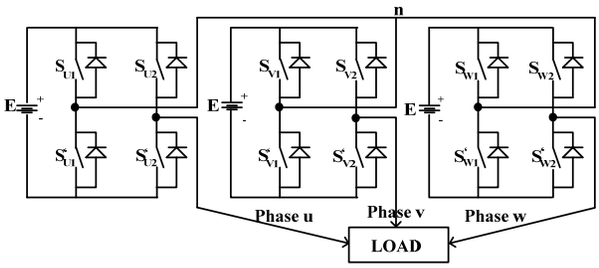

Figure 1. Three-phase three-level H-bridge inverter circuit

m is always an odd number in H-bridge multilevel inverter structure. The numbers of H-bridge are determined by considering the desired output voltage and harmonic contents [1, 6, 7].

$$H_{Bridge} = \frac{(m-1)}{2} \qquad (1)$$

In this paper, modeling and simulation of an H-bridge three-level inverter have been performed applying Sinusoidal Pulse Width Modulation (SPWM) and Space Vector Pulse Width Modulation (SVPWM) techniques with R-L and motor loads using Simulink/

[1] *Nevsehir H.B.V. University, Nevsehir, Turkey, akbilhan@nevsehir.edu.tr*
[2] *Firat University, Elazig, Turkey*

MATLAB package program. Comparison results of two methods are given respectively.

2. Analysis of SPWM Technique For Three-Level Inverter

In SPWM technique, Pulse Width Modulation (PWM) signals are generated by comparing a sinusoidal signal (reference signal magnitude is V_{Ref} and frequency f_{Ref}) with a triangle signal (carrier signal magnitude is $V_{carrier}$ and frequency f_C) [8]. To increase the number of output levels, number of carrier signal is increased keeping the reference signal. Number of carrier signal ($N_{carrier}$) and modulation index (M_i) are given in Eq. (2) and (3), respectively.

$$N_{carrier}=m-1 \quad (2)$$

$$M_i=\frac{\hat{V}_{Ref.}}{(a-1)\hat{V}_{Car.}} \quad (3)$$

The carrier signals and reference signals are compared as shown in Fig.2 in three-level SPWM.

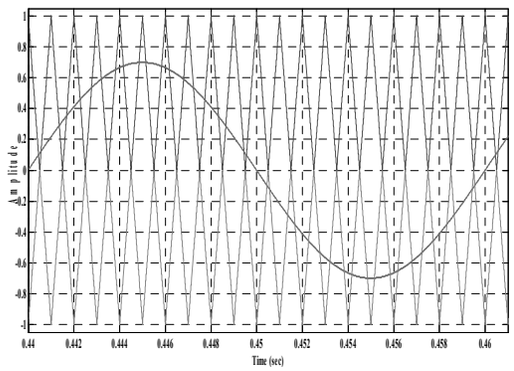

Figure 2. Three-Level SPWM

Analog implementation of this technique is hardly used now. Because, pulse widths are solutions to transcendental equations so that it is not suitable for microprocessor applications. Instead regular sampling is used where the reference signal is sampled and held at a frequency of fc or 2 fc. The sampled signal is then compared with the carrier signal. Interest in other PWM techniques has been also increased. Selective Harmonic Elimination PWM (SHEPWM) [9], minimum current ripple PWM, third harmonic injection PWM (THIPWM) [10] are some alternatives of the PWM techniques. However, space vector PWM (SVPWM) technique is recently showing popularity for inverter applications [1, 11-14].

3. Analysis of SVPWM Technique for Three-Level Inverter

Main aim of modulation techniques is to get less harmonic distortion, less switching losses and large modulation ratio. For this reason, many modulation techniques have been improved. Recently, SVPWM technique has become more popular because of achieving the goals mentioned above. Besides these advantages of SVPWM, it has some disadvantages such as complex calculation procedures [15, 16]. Switching states and active voltage levels can be calculated by using Eq. (4) and (5).

$$A=m^3 \quad (4)$$

$$A_{Active}=1+6\sum_{i=1}^{m-1} i \quad (5)$$

In each phase, there are four switching devices each having anti parallel diodes as shown in Fig.1. There are $3^3 = 27$ switching states for three-level H-bridge SVPWM. Every switching states can be represented as a voltage level by using Eq. (3). Three of them (111, 000, -1-1-1) are zero voltage vectors and they are centered in the middle of the space vector hexagon. Other switching states are active voltage vectors and they are located in the different part of hexagon. Possibilities for all switching states are given in Fig.3. Also switching states of the three-level inverter is listed in Table1. x represents u, w and z phases, respectively [15-17].

Table 1. Switching States of Three-Level Inverters (x=u, w, z phases)

S_{X0}	S_{X1}	S_{X2}	S'_{X1}	S'_{X2}
+E/2V	on	off	off	on
0V	on	on	off	off
0V	off	off	on	on
-E/2V	off	on	on	off

Fig.3 shows space vector diagram of the three-level inverter. As can be seen, the hexagon is divided into six portions and every portion is divided into four different parts. The portions are named as Sectors (Sector A, Sector B,…, Sector F) and four parts are named as region (Region 1,…, Region 4) [14, 18, 19].

Output voltage is produced by using three adjacent vectors. Eq. (8) shows how to calculate the output voltage, V*.

$$T_U V_U + T_V V_V + T_W V_W = T_S V^* \qquad T_U + T_V + T_W = T_S \tag{6}$$

where; T_S is the sampling time, V_U, V_V, and V_W are three adjacent vectors and T_U, T_V and T_W are vector duration times. Vector, V* falls into one of the six sectors depending on the vector angle, θ and it is calculated by using Eq. (7) and (8). V_α and V_β are used to determine the reference vector. The three-phase variables transforms to equivalent two-phase variables. Table 2 defines the sectors and their regions. [20-22].

$$V^* = V_\alpha + jV_\beta = \frac{2}{3}(V_U e^{j0} + V_V e^{\frac{j2\pi}{3}} + V_W e^{\frac{j4\pi}{3}}) \tag{7}$$

$$\theta = \arctan^{-1}\left(\frac{V_\beta}{V_\alpha}\right) \tag{8}$$

The other important issue is to estimate position of the voltage vector (V*) correctly. To achieve this, some geometrical equations illustrated in Fig.4 and given with Eq. (9-10) are used.

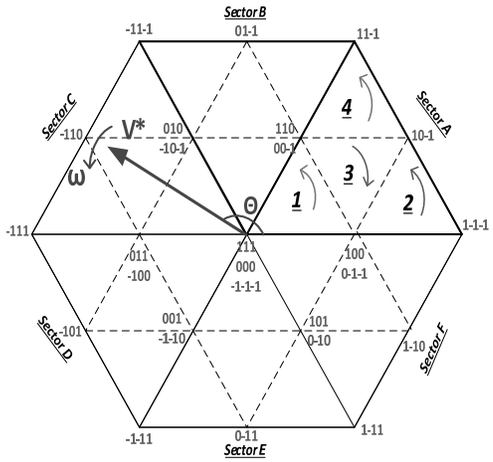

Figure 3. Space Vector Diagram of Three-Level Inverter

Table 2. V* Position in Three-Level SVPWM Diagram

Angle(Θ)	Sector
0° ≤ Θ < 60°	Sector A
60° ≤ Θ < 120°	Sector B
120° ≤ Θ < 180°	Sector C
180° ≤ Θ < 240°	Sector D
240° ≤ Θ < 300°	Sector E
300° ≤ Θ < 360°	Sector F

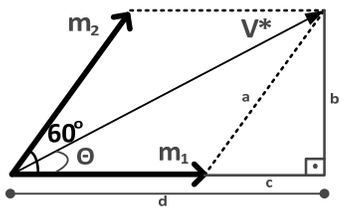

Figure 4. Estimating position of V*

$b = m_n \mathrm{Sin}\theta$ and $b = a\mathrm{Sin}\theta$

$$a = m_2 = \frac{b}{\mathrm{Sin}60} = \frac{2}{\sqrt{3}} b = \frac{2}{\sqrt{3}} V^* \mathrm{Sin}\theta \tag{9}$$

$m_1 = d - c$

$$m_1 = V^*\left(\mathrm{Cos}\theta - \frac{\mathrm{Sin}\theta}{\sqrt{3}}\right) \tag{10}$$

It is important to notice that only one switching device is at any time. The switching sequences for each region located in Sector A are given below using all switching states. "1" represents +E/2 V, "0" represents 0 V, and "-1" represents -E/2 V output voltage levels. Therefore, switching signals for Sector A are [14, 23, 24];

Region 1:-1-1-1, 0-1-1, 00-1, 000, 100, 110, 111, Region 2:0-1-1, 1-1-1, 10-1, 100, Region 3: 0-1-1, 00-1, 10-1, 100, 110, Region 4:00-1, 10-1, 11-1, 110,

Fig.5 shows switching states and times for Sector A [1, 14, 25].

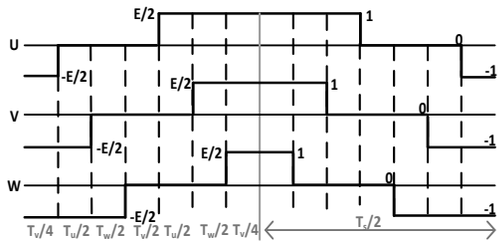

(a) Region 1

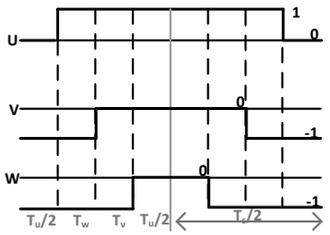

(b) Region 2

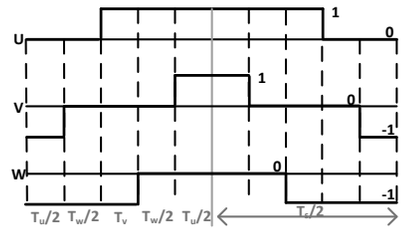

(c) Region 3

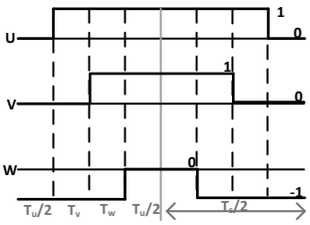

(d) Region 4

Figure 5. Switching signals of Sector A for all regions

For three-level SVPWM, space vector diagram and equations for switching times in Sector A is given in Fig.6 and Table 3, respectively.

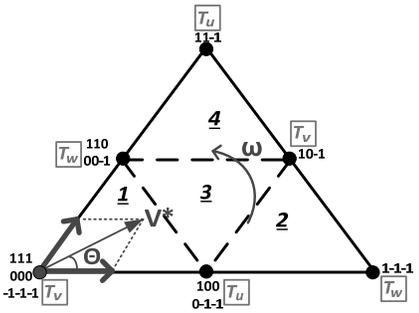

Figure 6. Space vector diagram of Sector A

Table 3. Switching Times and Equations of Sector A For Three-Level SVPWM

Switching Times	**Region 1**
T_u	$n*T_s*\sin((\pi/3)- \Theta)$
T_v	$T_s/2(1-(2*n*\sin(\Theta+\pi/3))$
T_w	$n*T_s*\sin \Theta$
	Region 2
T_u	$T_s(1-n*\sin(\Theta+\pi/3))$
T_v	$T_s*n*\sin \Theta$
T_w	$T_s/2((2*n*\sin(\pi/3-\Theta))-1)$
	Region 3
T_u	$T_s/2(1-2*n* \sin \Theta)$
T_v	$T_s/2(2*n*\sin(\pi/3+ \Theta)-1)$
T_w	$T_s/2(1+2*n*\sin(\Theta-\pi/3))$
	Region 4
T_u	$T_s/2(2*n*\sin(\Theta)-1)$
T_v	$n*T_s*\sin((\pi/3)- \Theta)$
T_w	$T_s(1-(n*\sin(\Theta+\pi/3))$

where n is constant. m_{SVPWM} is a modulation index of SVPWM and it is defined as;

$$m_{SVPWM}=\frac{\sqrt{3}}{2}\frac{V^*}{V_E} \qquad (11)$$

4. Modelling and Simulation

Fig.7 shows MATLAB/Simulink model of the whole system for both SPWM and SVPWM techniques. "A Phase", "B Phase" and "C Phase" blocks in Fig.7 contain H-bridge inverter structures. In these blocks, output voltages are synthesized. "E Source", "E Source1" and "E Source2" blocks are independent DC voltage source blocks. They are input to each H-bridge inverters and they are all isolated from each other. "Switching Signals of Phase A", "Switching Signals of Phase B" and "Switching Signals of Phase C" blocks produce switching signals using SPWM and SVPWM techniques as explained in the previous sections.

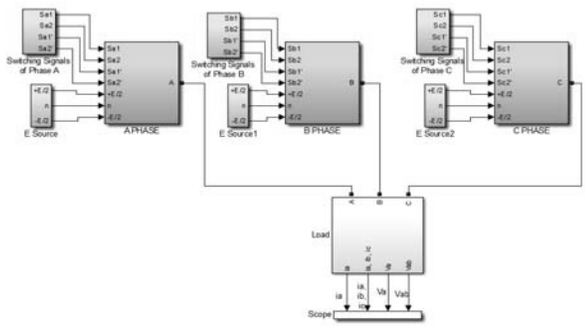

Figure 7. Simulation model of the whole system

In Fig.8 (a) and (b), basic structure of "Switching Signals of Phase" blocks applying SPWM and SVPWM techniques has been shown, respectively.

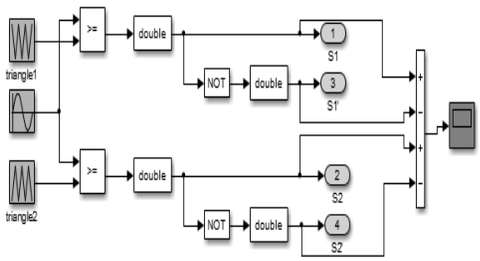

(a)

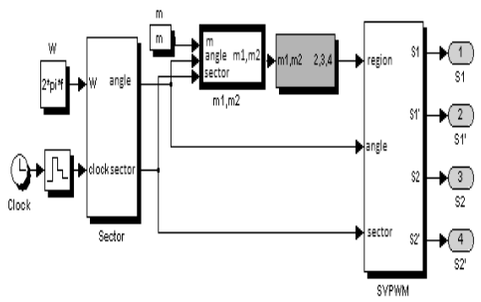

(b)

Figure 8. Producing Switching Signals (a) SPWM (b) SVPWM

Simulation results for both SPWM and SVPWM methods have been taken for various operating conditions. A passive load of R=100 Ω and L=0.1 H and motor load are used to demonstrate the performance of the inverter controlled by SPWM and SVPWM algorithms. The motor parameters are given in Appendix. Switching frequency of 1 kHz is used in the model. DC link voltage of the cascade inverters is taken as 500 V.

Simulation results shown in Fig.9 through Fig.11 have been obtained for modulation index of 0.2 and 0.8 and output frequency of 10 Hz, 30 Hz and 70 Hz for SPWM and SVPWM with passive load.

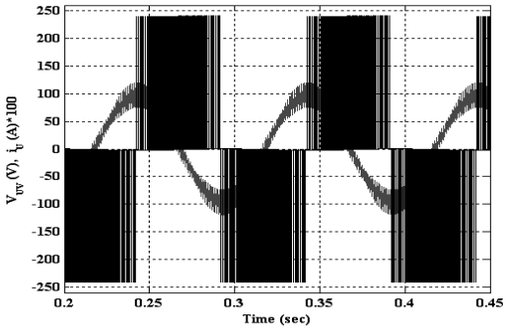

(a)

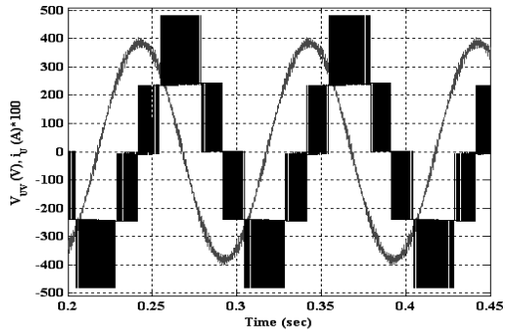

(b)

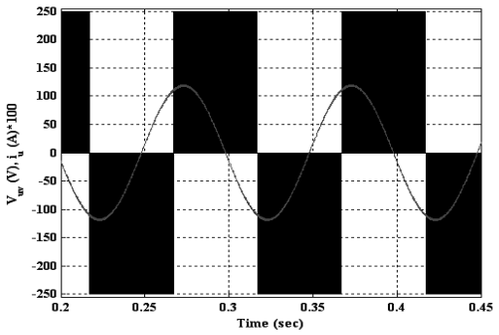

(c)

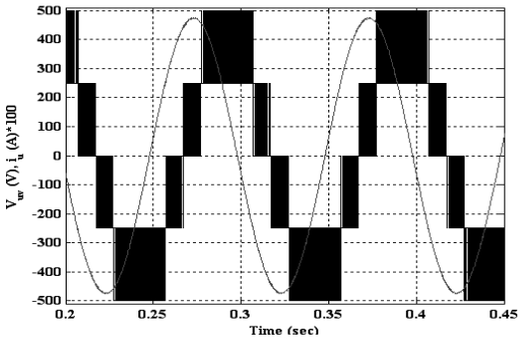

(d)

Figure 9. Simulation results of V_{ab} output line voltage and i_b phase current (x100) a) f=10 Hz and m=0.2 using SPWM,b) f=10 Hz and m=0.8 using SPWM, c) f=10 Hz and m=0.2 using SVPWM, d) f=10 Hz and m=0.8 using SVPWM for R=100 Ω, L=0.1 H passive load.

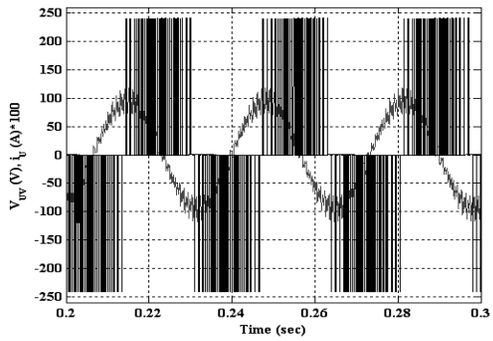

(a)

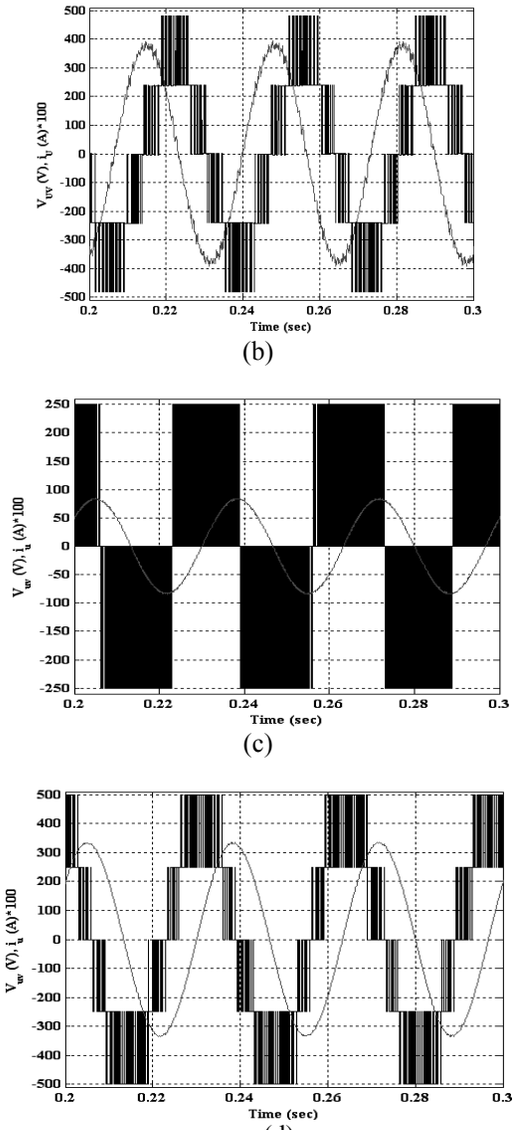

Figure 10. Simulation results of V_{ab} output line voltage and i_b phase current (x100) a) f=30 Hz and m=0.2 using SPWM,b) f=30 Hz and m=0.8 using SPWM, c) f=30 Hz and m=0.2 using SVPWM, d) f=30 Hz and m=0.8 using SVPWM for R=100 Ω, L=0.1 H passive load.

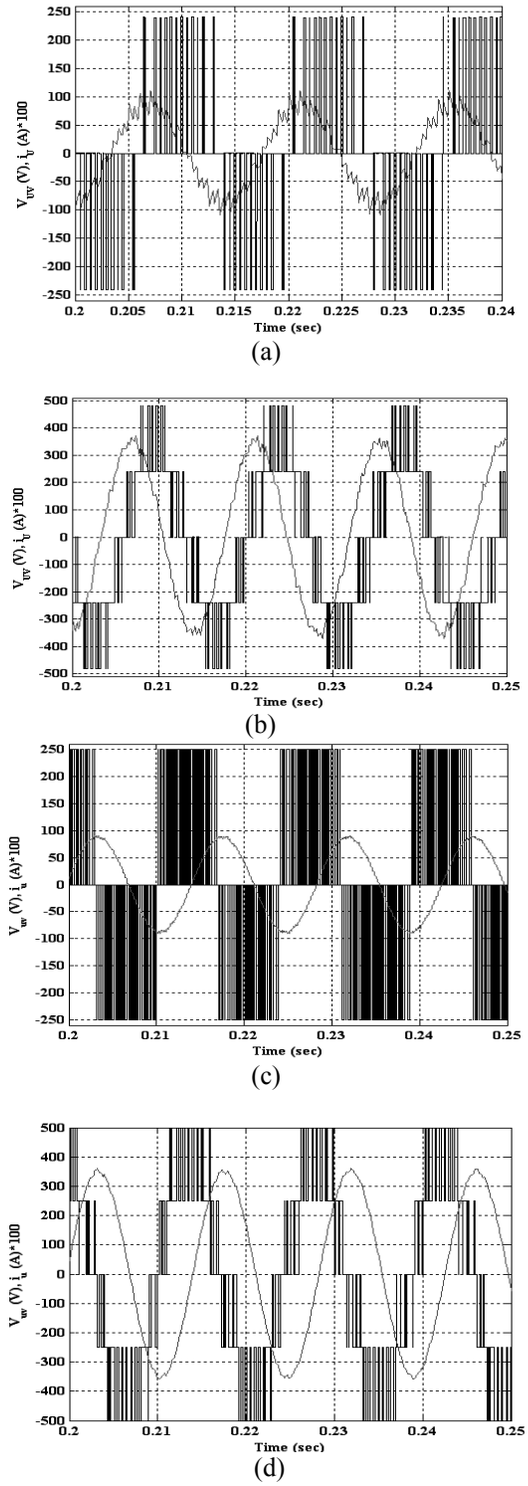

Figure 11. Simulation results of V_{ab} output line voltage and i_b phase current (x100) a) f=70 Hz and m=0.2 using SPWM, b) f=70 Hz and m=0.8 using SPWM, c) f=70 Hz and m=0.2 using SVPWM, d) f=70

Hz and m=0.8 using SVPWM for R=100 Ω, L=0.1 H passive load.

As can be seen from the results that the output voltage wave forms have three-level in lower modulation index of 0.2 and five-level in higher modulation index of 0.8.
As can be easily noticed that current waveforms with SVPWM have better sinusoidal shape for all conditions comparing to the current waveforms with SPWM. It can be also observed that operating range of SVPWM is higher than that of SPWM. As a result, SPWM uses bigger modulation index to get same output voltage as SVPWM. This is given in Eq.(12) as;

$$m_{SPWM} = \frac{4}{3} m_{SVPWM} \quad (12)$$

In Fig.12 and Fig.13, simulation of SVPWM has been repeated for an induction motor load. The results have been taken at no-load conditions. Fig.12 shows motor phase current of phase-u fed by the three-level SVPWM inverter at 10 Hz output frequency. Modulation index (m_{SVPWM}) is taken as 0.2 to provide constant v/f operation in steady-state.

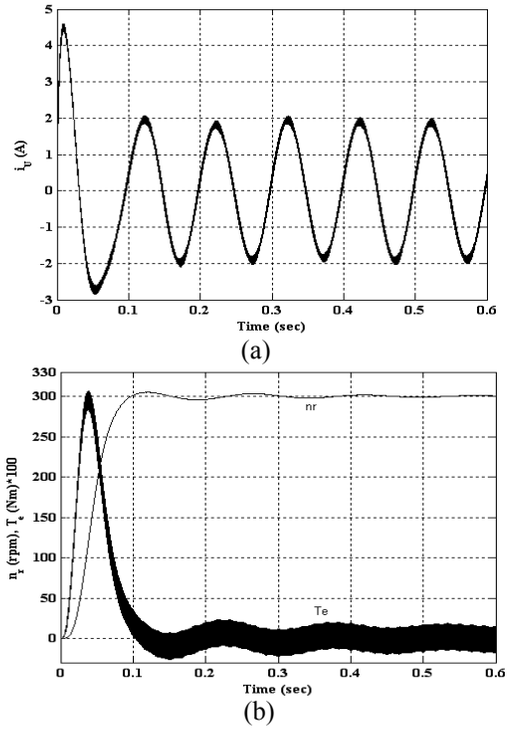

Figure 12. (a) Motor current waveform for phase-u, (b) Motor speed and electromagnetic torque for m=0.2 and f=10 Hz using SVPWM technique.

Fig.13 illustrates phase motor current and motor speed and torque waveforms for an output frequency of 70 Hz.

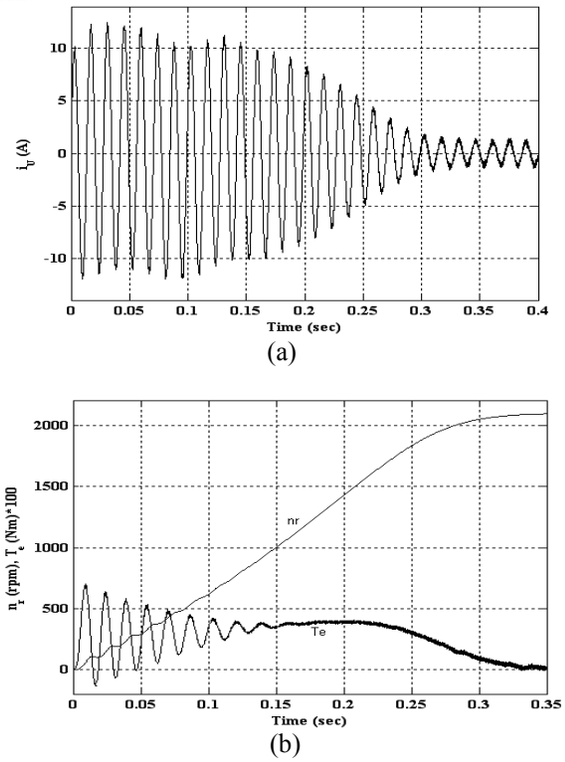

Figure 13. (a) Motor current waveform for phase-u, (b) Motor speed and electromagnetic torque for m=0.8 and f=70 Hz using SVPWM technique.

5. Conclusions

The space vector PWM method (SVPWM) and the sinusoidal PWM method (SPWM) for three level inverter using H-bridge topology have been modelled and simulated. Simulation results have been taken for R-L passive load and motor load for both methods. A proposed method (SVPWM) has shown better performance than classical conventional method (SPWM). From the results it is clear that, SVPWM gave less current ripple, THD than the SPWM modulation scheme. The proposed algorithm can be easily applied to multilevel inverters. It is more difficult to realize both digital and analog applications of SPWM method to multilevel inverters comparing to the SVPWM method. The proposed control algorithm given for the three-level inverter can be easily applied to multilevel inverters. It has been shown that high quality waveforms at the output of multilevel inverters can be reached by using proposed method.

Appendix

Ratings of the three-phase, 4-pole, 380 V, 50 Hz squirrel cage induction motor are:

Frequency range: 0-70 Hz, Stator resistance (Rs): 7 Ω, Rotor resistance (Rr): 6 Ω, Stator leakage inductance (Lσs): 0.52 mH, Rotor leakage inductance (Lσr): 0.52 mH, Magnetizing inductance (Lm): 0.5 mH, Rotor inertia (J): 0.0085 kgm^2, PN: 1.1 kW, TN: 7.62 Nm.

REFERENCES

[1] B.K., Bose, "Modern power electronics", 1983.

[2] J., Rodriguez, J.-S., Lai, F.Z., Peng, "Multilevel inverters: A survey of topologies, controls and applications", IEEE Trans. on Industrial Electronics, Vol. 49, No. 4, pp. 1631-1639, Aug. 2002.

[3] M., Manjrekar, G., Venkataramanan, "Advanced topologies and modulation strategies for multilevel inverters", Power Electronics Specialists Conference, Vol. 2, pp. 1013-1018, 23-27 June 1996.

[4] P.M., Bhagwat, V.R., Stefanovic, "Generalized structure of a multilevel inverter", IEEE Trans. on I.A., Vol. IA-19, n.6, pp. 1057-1069, 1983.

[5] N., Mohan, T.M., Undeland, W.P., Robbins, "Power electronics: converters, applications, and design", John Wiley & Sons, Inc., 1989.

[6] A.K., Gupta, A.M., Khambadkone, "A space vector pwm scheme for multilevel inverters based on two-level space vector pwm", IEEE Trans. on Industrial Electronics, Vol. 53, No. 5, Oct. 2006.

[7] G., Guo, W., You, "Quality analysis of svpwm inverter output voltage", IEEE International Conference on Computer Science and Software Engineering, pp. 126-129, 2008.

[8] C.S.Sharma, T., Nagwani, "Simulation and Analysis of PWM Inverter Fed Induction Motor Drive", Int. J. of Science, Engineering and Technology Research, Vol. 2, No. 2, pp. 359-366, 2013.

[9] B.P., McGrath, D.G., Holmes, "A comparison of multicarrier pwm strategies for cascaded and neutral point clamped multilevel inverters" IEEE Power Electronics Specialists Conference, Vol. 2, pp.674 – 679, 18-23 June 2000.

[10] W., Subsingha, "A Comparative Study of Sinusoidal PWM and Third Harmonic Injected PWM Reference Signal on Five Level Diode Clamp Inverter", Energy Procedia, Vol. 89, pp. 137-148, 2016.

[11] M.S.A., Dahidah, G., Konstantinou, V.G. Agelidis, "A Review of Multilevel Selective Harmonic Elimination PWM: Formulations, Solving Algorithms, Implementation and Applications", IEEE Trans. on Power Electronics, Vol. 30, No. 8, pp. 4091-4106, 2015.

[12] C., Zang, Z., Pei, J., He, T., Guo, J., Zhu, W., Sun, "Research on the application of CPS-SPWM technology in cascaded multilevel inverter", International Conference Electrical Machines and Systems, ICEMS, pp. 1-4, 2009.

[13] J., Pradeep, R., Devanathan, "Comparative analysis and simulation of pwm and svpwm inverter fed permanent magnet synchronous motor", International Conference on Emerging Trends in Electrical Engineering and Energy Management (ICETEEEM), pp. 299-305, 2012.

[14] A., Kocalmis, S., Sunter, "Simulation of a space vector pwm controller for a three-level voltage-fed inverter motor drive", IECON 2006-32nd Annual Conference on IEEE Industrial Electronics, pp. 1915–1920, 6-10 Nov. 2006.

[15] R., Rabinovici, D., Baimel, J., Tomasik, A., Zuckerberger, "Series space vector modulation for multi-level cascaded H-bridge inverters", Power Electronics, IET., pp. 843–857, 2010.

[16] J.H., Seo, C.H., Choi, D.S., Hyun, "A new simplified space–vector pwm method for three-level inverters", IEEE Trans. on Power Electronics, Vol. 16, No. 4, pp. 545-550, July. 2001.

[17] N., Celanovic, D., Boroyevich, "A fast space–vector modulation algorithm for multilevel three–phase converters", IEEE Transactions on Industry Applications, Vol. 37, No. 2, pp. 637–641, March/April 2001.

[18] L., Chengwu, Z., Xiaomin, J., Qiguang, "Research on SVPWM inverter output control technology", Fifth Conference on Measuring Technology and Mechatronics Automation, pp. 927-929, 2013.

[19] A.K., Gupta, A.M., Khambadkone, "A space vector modulation scheme to reduce common mode voltage for cascaded multilevel inverters", IEEE Trans. Power Electronic, Vol. 22, No. 5, pp. 1672–1681, Sep. 2007.

[20] S.K., Mondal, B.K., Bose, V., Oleschuk, J.O.P., Pinto, "Space vector pulse width modulation of three-level inverter extending operation into overmodulation region", IEEE Trans. on Power Electronics, Vol.18, pp.604 – 611, March 2003.

[21] O., Aydogmus,"Design of a solar motor drive system fed by a direct-connected photovoltaic array", Advances in Electrical and Computer Engineering, Vol.12, n. 3, pp. 53-58, 2012.

[22] Y.-H., Lee, B.-S., Suh, C.-H., Choi, D.-S., Hyun, "A new neutral point current control for a 3-level

converter inverter pair system", Industry Applications Conference, Thirty-Fourth IAS Annual Meeting, Vol.3, pp. 1528-1534, 1999.

[23] G., Shiny, M.R., Baiju, "A low computation space vector pwm scheme for multilevel inverters based on fractal approach", IEEE Symposium on Industrial Electronics & Applications (ISIEA), pp. 131–136, 2010.

[24] S.N., Rao, D.V.A., Kumar, C.S., Babu, "New multilevel inverter topology with reduced number of switches using advanced modulation strategies", 2013 International Conference on Power, Energy and Control (ICPEC), pp. 693-699, 2013.

[25] K., Jinsong, C., Yu, W., Haifeng, N., Yichuan, "Three-level inverter speed sensorless system with field orientation control", 2012 IEEE 7th International Power Electronics and Motion Control Conference - ECCE Asia, June 2-5, Harbin, China, 2012.